Intrinsic Limits on the Detection of the Anisotropies of the Stochastic Gravitational Wave Background

Giorgio Mentasti and Carlo R. Contaldi
Blackett Laboratory, Imperial College London, SW7 2AZ, London, United Kingdom

Marco Peloso
Dipartimento di Fisica e Astronomia "Galileo Galilei", Università di Padova, 35131 Padova, Italy and INFN, Sezione di Padova, 35131 Padova, Italy

(Received 26 January 2023; revised 19 July 2023; accepted 31 October 2023; published 30 November 2023)

For any given network of detectors, and for any given integration time, even in the idealized limit of negligible instrumental noise, the intrinsic time variation of the isotropic component of the stochastic gravitational wave background (SGWB) induces a limit on how accurately the anisotropies in the SGWB can be measured. We show here how this sample limit can be calculated and apply this to three separate configurations of ground-based detectors placed at existing and planned sites. Our results show that in the idealized, best-case scenario, individual multipoles of the anisotropies at $\ell \leq 8$ can only be measured to $\sim 10^{-5}$–10^{-4} level over five years of observation as a fraction of the isotropic component. As the sensitivity improves as the square root of the observation time, this poses a very serious challenge for measuring the anisotropies of SGWB of cosmological origin, even in the case of idealized detectors with arbitrarily low instrumental noise.

DOI: 10.1103/PhysRevLett.131.221403

Introduction.—The field of gravitational wave (GW) detection has flourished in recent years following the first observation of the signal from merging, massive, compact systems [1]. Many more detections have been made since the sensitivity of the existing LIGO-Virgo-KAGRA network continues to improve [2]. The sensitivity of existing networks is expected to keep improving in the coming decades, and new ground-based detectors are already being planned [2,3]. While an increasingly large number of astrophysical signals arising from compact binary coalescence events have been observed, we are still awaiting the detection of a stochastic gravitational wave background (SGWB). The latest observations by LIGO-Virgo-KAGRA [2] place upper limits $\Omega_{\rm GW} \lesssim 5.8 \times 10^{-9}$ and $\Omega_{\rm GW} \lesssim 3.4 \times 10^{-9}$ for, respectively, a scale-invariant and a stochastic signal from astrophysical sources with a power law spectral index of $2/3$, pivoted at 25 Hz [4,5].

The SGWB is expected to be both of astrophysical and cosmological origin. The astrophysical component originates from the superposition of a large number of unresolved sources, with the dominant contribution (at frequencies probed by ground-based detectors) from the coalescence of black holes and neutron star binaries. The cosmological component is more uncertain, possibly originating in nonminimal models of inflation, phase transitions, and topological defects [6–8].

The simplest way to disentangle these two components is through the frequency dependence of $\Omega_{\rm GW}$, the amplitude of the isotropic component of the SGWB [8]. Any anisotropy in the SGWB will also be of interest for the separation into different components. In particular, any directional dependence will assist in distinguishing between galactic and extragalactic components and to search for any correlation with known tracers of structure [9–16]. Anisotropies in the astrophysical background are expected to be correlated with the large scale structure, due to both how the GW originate and on how they propagate through a perturbed universe [10,17,18]. Cosmological backgrounds, along with astrophysical ones in the limit of confused, persistent sources [19], can be modeled as stationary phenomena. We will focus on this stationary limit in this work.

This Letter describes the application of a method developed for studying the signal-to-noise ratio (SNR) of anisotropies in SGWBs as observed by a network of detectors [20]. We consider observations by a network of detectors placed at the location of existing (two LIGOs, Virgo and KAGRA [21–23]) and proposed [Einstein Telescope (ET) and Cosmic Explorer (CE) [24,25]] instruments. Differently from the existing literature, here, for the first time, we investigate the "noiseless limit" of idealized instruments, where the sample variance of the observations dominates the error. Namely, we study the best-case scenario in which the noise of the instruments will be reduced to an arbitrarily low level. We find that, even in this ideal limit, it is impossible to achieve arbitrary resolution in the measurement of anisotropies in the background because of the intrinsic variance of its *isotropic* component.

For simplicity, we consider an unpolarized and Gaussian SGWB, whose variance has a factorized dependence on the frequency f and on the direction of observation $\hat{n}$

$$\langle h^{*}(f,\hat{n})h(f,\hat{n})\rangle = \frac{3H_0^2}{32\pi^3 f^3}\Omega_{\rm GW}(f)\sum_{\ell m}\delta_{\ell m}^{\rm GW}Y_{\ell m}(\hat{n}), \quad (1)$$

where H_0 is the Hubble constant. Integrating this relation over the full sky, only the monopole term survives, and, for $\delta_{00}^{\rm GW}=\sqrt{4\pi}$, the parameter $\Omega_{\rm GW}(f)$ is the fractional relative energy in GW per log frequency, $\Omega_{\rm GW}=(d\rho_{\rm GW}/d\log f)/\rho_c$ [26], where $\rho_{\rm GW}(f)$ is the energy density of the SGWB, and ρ_c is the critical energy density. The coefficients $\delta_{\ell m}^{\rm GW}$ quantify the relative energy density in a multipolar expansion (Our definition is in agreement with that of [8].) relative to that of the monopole. The expansion is done in analogy to that used in maps of the cosmic microwave background (CMB) radiation.

We assume that the anisotropy is much weaker than the monopole, i.e., $|\delta_{\ell m}^{\rm GW}|\ll 1$, which is reasonable for both the cosmological and the astrophysical models, and that the $\hat{z}$ axis chosen to define the $Y_{\ell m}$ harmonic functions is aligned with the Earth rotation axis.

Methodology.—We consider N ground-based GW interferometers labeled by indices $i,j=1,2,\ldots,N$. An SGWB results in a time-dependent signal $s_i(t)$ in each of the instruments that depend on the response, the location, and the orientation of their arms (see, e.g., [20,27]). The signal is proportional to the difference in travel time of photons that propagate through different arms of the detector and that would travel in an identical amount of time in the absence of a GW through the detector. The detectors are also affected by instrumental noise $n_i(t)$, such that each instrument measures the data stream

$$m_i(t)=s_i(t)+n_i(t). \quad (2)$$

Following the formalism of [20,27] we Fourier-transform the data streams obtained in pairs of detectors i and j over a time window τ centered at t, and build the observable $\mathcal{C}_{ij}(f,t)$ by cross-correlating them,

$$\mathcal{C}_{ij}(f,t)\equiv m_i^{\star}(f,t)m_j(f,t), \qquad i\neq j. \quad (3)$$

The $i\neq j$ specification indicates that correlations need to be taken between different (and well-separated) sites so that the expectation value of the correlation of the noise between the two sites vanishes. In this way, only a GW passing through both sites correlates the two measurements, and the expectation value of the cross correlator between the two data streams, therefore, provides an unbiased estimator of the signal. Taking advantage of the Earth rotation, we can compress the $\mathcal{C}_{ij}(f,t)$ into a set of functions $\mathcal{C}_{ij,m}(f)$ obtained through a finite-length, Fourier transform along the Earth rotation axis in a total observation time T

$$\mathcal{C}_{ij,m}(f)\equiv\frac{1}{T}\int_0^T dt\, {\rm e}^{-2\pi imt/T_e}\mathcal{C}_{ij}(f,t), \quad (4)$$

where T_e is the period of rotation of the Earth. The index m is an integer, and the coefficients $\mathcal{C}_{ij,m}(f)$ are the Fourier coefficients of the series reproducing the time-dependent function $\mathcal{C}_{ij}(f,t)$. We can integrate over frequency by applying a set of optimal filters $Q_{ij,m}(f)$, i.e., functions that can be chosen to maximize the signal-to-noise ratio (SNR) of any given estimate. This is the ratio between the expectation value of the measured $\mathcal{C}_{ij}$ and the square root of its variance. The latter provides, therefore, the forecast error of the measurement, and the main goal of this Letter is to single out a contribution to the variance that is present also in the limit of ideal, noiseless detectors, and that is related to the intrinsic variance of the dominant isotropic component of the signal. Namely, we define

$$\mathcal{C}_{ij,m}\equiv\int_{-\infty}^{\infty}df\,\mathcal{C}_{ij,m}(f)Q_{ij,m}(f). \quad (5)$$

For uncorrelated noise between different detectors, the expectation value $\langle\mathcal{C}_{ij}\rangle$ only contains contributions from the parametrized signal (1), i.e.,

$$\langle\mathcal{C}_{ij,m}\rangle\propto\int_{-\infty}^{\infty}df\,H(f)\sum_{\ell}\delta_{\ell m}^{\rm GW}\gamma_{ij,\ell m}(f)Q_{ij,m}(f), \quad (6)$$

where $\gamma_{ij,\ell m}(f)$ are the response functions that depend on the geometry of the two detectors i and j, on their distance vector, and on the multipole considered [20,27].

For definiteness, we assume that the special shape of the signal is characterized by a constant $\Omega_{\rm GW}(f)=\Omega_0$, and assume the fiducial value $\hat{\Omega}_0=10^{-9}$ in our explicit evaluations. However, due to the factorization (1) and the assumption of negligible instrumental noise, the accuracy in reconstructing the relative amplitudes $\delta_{\ell m}^{\rm GW}$ is independent of the level and functional form of $\Omega_{\rm GW}(f)$, as they cancel in the SNR under the assumption of negligible noise. Consequently, the result we present below for the assessment of the relative contribution of the anisotropic signal is independent of the amplitude and frequency shape of the dominant isotropic contribution. Furthermore, consistent with our goal of providing the best possible level with which any given multipole can be reconstructed, we assume that the signal is dominated by a monopole and a single anisotropic multipole, i.e., $\langle h^*(f,\hat{n})h(f,\hat{n})\rangle = \Omega_0 f^{-3}[1+\delta^{\rm GW}_{\ell m}Y_{\ell m}(\hat{n})]$ (This means that we have to be careful when treating the search of a multipole (ℓ, m) with $m=0$. The analysis can also be done in this case, but the method is slightly different [28].), as the simultaneous presence of more non-vanishing anisotropic coefficients can only worsen our accuracy in measuring each of them. We consider the log-likelihood function $\ln\mathcal{L}(\Omega_0,\delta^{\rm GW}_{\ell m}) \sim -\chi^2(\Omega_0,\delta^{\rm GW}_{\ell m})/2$ for the distribution of parameters relative to fiducial values $\hat{\Omega}_0$ and $\hat{\delta}^{\rm GW}_{\ell m}$ with

$$\chi^2 = \sum_{m'm''}\sum_{\substack{i\neq j\\ k\neq l}} r^\star_{ij,m'}\Sigma^{-2}_{ij,kl,m'm''}r_{kl,m''},$$

$$r_{ij,m'}(\Omega_0,\delta^{\rm GW}_{\ell m}) \equiv \mathcal{C}_{ij,m'}(\Omega_0,\delta^{\rm GW}_{\ell m}) - \left\langle \mathcal{C}_{ij,m'}(\hat{\Omega}_0,\hat{\delta}^{\rm GW}_{\ell m})\right\rangle,$$

$$\Sigma^2_{ij,kl,m'm''} = \langle r^\star_{ij,m'}r_{kl,m''}\rangle, \tag{7}$$

where we recognize the SNR structure (with the square of the difference between the actual and expected measurement at the numerator and the variance at the denominator). The likelihood provides the probability that (due to its variance) the measurement results in the values Ω_0 and $\delta^{\rm GW}_{\ell m}$, given an injected signal characterized by the "fiducial" values $\hat{\Omega}_0, \hat{\delta}^{\rm GW}_{\ell m}$. The probability is maximum at the fiducial values, and it then decreases with a Gaussian profile determined by the likelihood (7). The assumption of a Gaussian likelihood is justified by the fact that the estimators $\mathcal{C}_{ij,m}$ are obtained by averaging over a large number of frequencies and solid angles. Therefore we can assume that the central limit theorem holds. The assumption of small anisotropy, $|\delta^{\rm GW}_{\ell m}| \ll 1$, further simplifies the computation of the covariance term in (7). In a companion paper [28] we show that, after optimizing the filters $Q_{ij,m}(f)$, the chi-squared in (7) can be written, in compact form, as

$$\chi^2_{\rm opt} = T\left[\left(\frac{\Omega_0}{\hat{\Omega}_0}-1\right)^2 I_{00} + \frac{1}{4\pi}\left|\frac{\Omega_0}{\hat{\Omega}_0}\delta^{\rm GW}_{\ell m} - \hat{\delta}^{\rm GW}_{\ell m}\right|^2 I_{\ell m}\right], \tag{8}$$

where the coefficients $I_{\ell m}$ are calculated from the integration over frequency of the response functions of the network of instruments over the variance term. In the signal-dominated regime [i.e., when we can neglect the noise contribution and therefore set $n_i = 0$ in (2)], the variance term just depends on a combination of the response functions to the monopole of the various pairs of detectors in the network. Therefore, in this limit the coefficients I_{00} and $I_{\ell m}$ just depend on the geometry of the network and the orientation of the arms of the interferometers [28]. This regime allows us to determine what the ultimate limitations of a particular configuration of detectors will be in reconstructing the anisotropies of the SGWB.

We can now ask ourselves the question; *what is the detection threshold for an anisotropy in the signal-dominated regime?* Given the Gaussian assumption for the likelihood, we can forecast the expected error in a determination of parameters Ω_0 and $\delta^{\rm GW}_{\ell m}$ given their fiducial values $\hat{\Omega}_0$, $\hat{\delta}^{\rm GW}_{\ell m}$. We do so by expanding the expression (8) to quadratic order in the departure of the parameters from their fiducial values, namely, by computing the second derivatives of (8), which form the so-called Fisher matrix. To estimate the detection threshold, we choose $\hat{\delta}^{\rm GW}_{\ell m} = 0$, in which case the Fisher matrix is diagonal in the two parameters Ω_0 and $\delta^{\rm GW}_{\ell m}$:

$$\chi^2_{\mathcal{F}} = T\left[\left(\frac{\Omega_0}{\hat{\Omega}_0}-1\right)^2 I_{00} + \frac{1}{4\pi}|\delta^{\rm GW}_{\ell m}|^2 I_{\ell m}\right]. \tag{9}$$

This sets up a test for the rejection of the null hypothesis (no anisotropy), as we discuss below.

The calculation of the integral measures $I_{\ell m}$ in (9), in a general case, is complicated by the rotation of the network with respect to the sky, gaps in the data stream, and the presence of nonideal noise features. In the signal-dominated regime, assuming $|\delta^{\rm GW}_{\ell m}| \ll 1$, and aligning the coordinate frame (and thus the definition of $\delta^{\rm GW}_{\ell m}$) with the Earth rotation, the calculation can be significantly simplified and carried out analytically [28]. Since we wish to consider the most idealized case, where we have a single anisotropic multipole (ℓ, m) on top of a dominant monopole, we have that the only nonvanishing expectation values of (6) are $\langle\mathcal{C}_{ij,0}\rangle$ and $\langle\mathcal{C}_{ij,m}\rangle$. We note that in (9) the off-diagonal element of the Fisher matrix vanishes. This means that the observables $\mathcal{C}_{ij,m}$ with different values of m are uncorrelated. This is due to the fact that we have arbitrarily chosen in (1) to expand the anisotropies along the rotation axis of the Earth. The most general case, where one wishes to define the spherical harmonics expanded anisotropies with another axis, would lead to nondiagonal terms and, therefore, an even larger sample variance.

Results.—We apply the estimate to three cases. The first is "LVK," a network consisting of instruments at the two LIGO, the Virgo, and the KAGRA sites [21–23]. The second case, "LVK + ET" adds a triangularly shaped detector located at the proposed Sardinia site [24] for the Einstein Telescope. The third case, "CE + ET" consists of Cosmic Explorer and Einstein Telescope baselines only. We locate CE at the LIGO Hanford site. Consistently with the above discussion, we assume the signal-dominated regime across all detectors (namely, that the noise of all the instruments gives negligible contribution to the variances of the measurements). Throughout, we assume that data streams are Fourier transformed on a short timescale $\tau = 30$ sec. This ensures that the sky rotation is negligible during this time window, given the resolution of the detectors. We assume a total observation time of

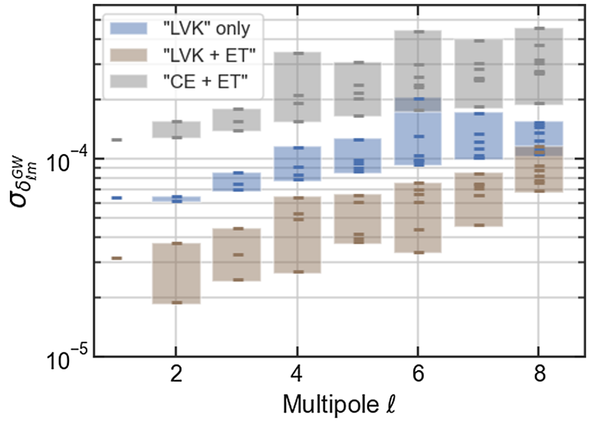

FIG. 1. Forecast errors induced by the intrinsic variance of the dominant isotropic component in the measurement of the multipolar coefficients $\delta^{\rm GW}_{\ell m}$, for each $\ell \leq 8$. These coefficients, introduced in Eq. (1), quantify the amplitude of the corresponding multipole of the SGWB relative to the isotropic component Ω_0. The shaded bands highlight the range of $\sigma_{\delta^{\rm GW}_{\ell m}}$ at each ℓ (with m spanning the range $-\ell$ to $+\ell$). A measured value of $\delta^{\rm GW}_{\ell m}$ above the value in the figure would signify a "detection" of that anisotropy mode at 68% C.L. Adding ET to the LVK network reduces sample variance at all multipoles, while CE + ET has worse sample variance.

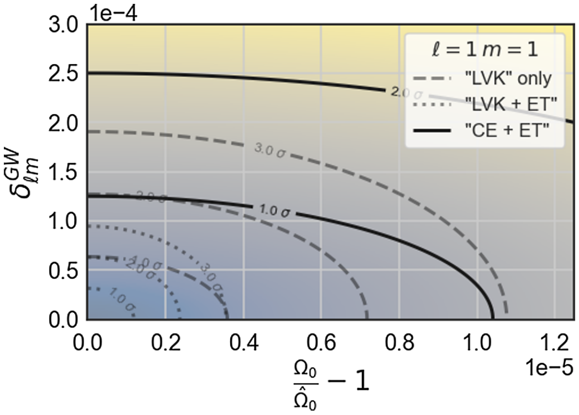

FIG. 2. The $\chi^2_{\mathcal{F}}$ contours in the plane of Ω_0 (the overall amplitude of the GW logarithmic energy density) and $\delta^{\rm GW}_{11}$ [one of the dipolar coefficients of the anisotropic expansion of the SWGB as defined in Eq. (1)]. The 1σ to 3σ contours are highlighted for both LVK and LVK + ET networks. The two parameters are uncorrelated for the choice of frame and variable definition adopted here.

$T = 5$ yr. We also assume a constant window in the frequency domain with $f \in [1, 1000]$ Hz. Although the scenario used here is not band limited by any noise filtering, this range mimics an optimistic frequency range of sensitivity for typical ground-based detectors. In practice, the effective window and bandwidth of the estimate will be determined by noise weighting. These assumptions, along with the coordinate alignment and noiseless limit, mean that our estimates constitute extreme *best-case*, sample limited scenarios for each chosen configuration.

In Fig. 1, we show, for each network and for each multipole ℓ (up to and including $\ell = 8$), the estimated standard deviation $\sigma_{\delta^{\rm GW}_{\ell m}} \equiv (T I_{\ell m}/4\pi)^{-1/2}$ as obtained after marginalizing (namely, after integrating the likelihood) over Ω_0, which provides an indication of the SNR = 1 threshold for detection of the SGWB anisotropy. Given that, as mentioned above Eq. (9), the fiducial signal in our analysis is isotropic, the values shown in the figure are the 68% confidence level (C.L.) forecast of what will be measured by the corresponding network if the SGWB is indeed isotropic. A measurement above this value will indicate that the hypothesis of isotropy is rejected at 68% C.L. Consequently, this value is our estimate of how large an anisotropy needs to be in order to be detected at this C.L. It is important to remember that the distribution of error amplitudes for a given multipole will change depending on the orientation of the coordinate frame, but the overall amplitude will be unchanged. In particular, the results show how the addition of baselines becomes important in the signal-dominated regime.

In Fig. 2 we show the function $\chi_{\mathcal{F}}$ evaluated around the fiducial values in $\hat{\Omega}_0$ and $\hat{\delta}^{\rm GW}_{\ell m} = 0$ (for one example choice of ℓ and m). The region within (outside) a given contour indicates the values for which a measurement is compatible (incompatible) with the fiducial values at the corresponding C.L. As discussed below Eq. (6), the result shown is independent of the fiducial value of Ω_0. This result also shows that the dominant effect, as expected in the absence of instrumental noise, is the number of baselines in the network.

The results show that even in the extreme case of a future ground-based network with negligible noise, the SNR = 1 threshold for the relative anisotropies is $\sim 10^{-5}$–10^{-4} over a period of measurement of $\mathcal{O}(10)$ yr. This scale is determined by the effective bandwidth Δf of the overlap functions, which is of the order of ~ 100 Hz, and the total integration time R, which is of the order of 10^8 s. This crude estimate gives $\sigma \propto (1/\sqrt{T \Delta f}) \sim 10^{-5}$ which reproduces well the scale of the sample variance, with an additional factor of ~ 1–10 (varying for the different networks considered) arising from the specific values of the function in the integrand of Eq. (9) [28]. We stress that improving the 10^{-5}–10^{-4} threshold by a factor of 10 requires increasing the measurement time by a factor of 100. Large angular scale anisotropies in the primordial background generated by the GW propagation in the early universe are expected to be below this level [6,29], with quadrupole amplitude $\sqrt{C_2} \sim 3 \times 10^{-5}$ [8]. Grater anisotropies in the cosmological SGWB are possible in specific contexts, for instance, in the presence of large primordial non-Gaussianity [30,31] or isocurvature modes [32,33]. Moreover, astrophysical backgrounds can be estimated to be of the order of 10^{-2} and are expected to have background amplitudes within reach of future sensitivity [10,17,34,35].

Another signal to consider is the kinematic dipole of the SGWB induced by the proper motion of the Earth with respect to the background [36]. This signature is analogous to the dipole observed in the CMB radiation. The statement that the observed universe is homogeneous and isotropic at large scales applies only to one specific frame, denoted as the CMB rest frame. The large dipole in the CMB indicates [37] that the solar system is moving in this frame, with proper velocity $v/c \sim 1.2 \times 10^{-3}$, in the direction of galactic coordinates ($l = 264°$, $b = 48°$). The cosmological SGWB also has its rest frame, and it is reasonable to assume that it coincides with that of the CMB (assuming, for instance, that both signals originate from cosmological distances where the homogeneous limit applies). Future SGWB measurements might allow us to test this assumption. The observed CMB kinematic dipole translates to an expected dipolar SGWB anisotropy with coefficients $\delta^{\mathrm{GW}}_{1,-1} = -\delta^{\mathrm{GW}}_{1,1} \simeq \sqrt{(2\pi/3)}\beta$ [20]. As proved in [28], the variance in the measurement of any given $\delta^{\mathrm{GW}}_{\ell,m}$ is independent of the sign of m. Therefore, the combined measurement of the two multipoles allows us to have a final uncertainty on the kinematic dipole of $\sigma_\beta = \sqrt{(3/4\pi)}\sigma_{\delta^{\mathrm{GW}}_{1,1}}$. This evaluates to $\sigma_\beta = 3.4 \times 10^{-5}$ for the LVK network and $\sigma_\beta = 1.6 \times 10^{-5}$ with the addition of ET. Therefore, sample variance is not an obstacle to detecting the kinematic dipole induced by our peculiar motion under the assumption that the SGWB rest frame coincides with the CMB one.

Conclusions.—We have studied the impact of the intrinsic variance of the monopole on the measurement of the ansotropies of the SGWB. This term adds up to the instrumental noise [28]. To assess the relative importance of the two contributions, let us consider as an example the specific case of the measurement of a scale-invariant dipole ($\ell = m = 1$). In this case, the sample variance component amounts to $\simeq 7 \times 10^{-5}$ of the total variance for the existing LVK network at design sensitivity. As detectors will improve, the sample variance will become more important, contributing with $\simeq 5 \times 10^{-4}$ of the total uncertainty for the LVK + ET network and to $\simeq 0.14$ for the ET + CE network. Similar results are obtained for different multipoles, as can be deduced from the results shown in Fig. 4 of Ref. [28]. In providing these values, we have assumed that Ω_0 saturates its current upper bound [2]. The weight of the intrinsic variance relative to the instrumental noise is directly proportional to Ω_0 [28], and therefore we expect it to be relevant in future measurements for the level of the isotropic signal that can be expected for the astrophysical backgrounds and some cosmological scenarios [6].

The results presented in this Letter focus on the best-case scenario of detectors with negligible instrumental noise, showing that, in this idealized limit, several network configurations of existing and planned interferometers achieve SNR = 1 at 10^{-5}–10^{-4} in the amplitudes $\delta^{\mathrm{GW}}_{\ell,m}$ (relative to the monopole) of the multiples of the SWGB. This best-case scenario also assumed that only one multipole of the anisotropy is present, and so it disregards correlations between different multipoles that are generally expected to be present. Given the complicated and noncompact sky response functions of interferometer networks, we should expect these correlations to be significant. This underscores that our estimates should be considered the most optimistic lower bounds on the sample variance of individual anisotropies.

We thank Vuk Mandic for useful discussions. M. P. is supported by Istituto Nazionale di Fisica Nucleare (INFN) through the Theoretical Astroparticle Physics (TAsP) and the Inflation, Dark Matter and the Large-Scale Structure of the Universe (InDark) project. G. M. acknowledges support by the Imperial College London Schrödinger Scholarship scheme. C. R. C. acknowledges support under a UKRI Consolidated Grant No. ST/T000791/1.

[1] B. P. Abbott, R. Abbott, T. D. Abbott, M. R. Abernathy, F. Acernese, K. Ackley, C. Adams, T. Adams, P. Addesso, R. X. Adhikari *et al.* (LIGO Scientific Collaboration and Virgo Collaboration), Phys. Rev. Lett. **116**, 061102 (2016).
[2] R. Abbott *et al.* (LIGO Scientific Collaboration, Virgo Collaboration, and KAGRA Collaboration), Phys. Rev. D **104**, 022004 (2021).
[3] R. Abbott *et al.* (LIGO Scientific Collaboration, Virgo Collaboration, and KAGRA Collaboration), Phys. Rev. D **104**, 022005 (2021).
[4] T. Regimbau, Res. Astron. Astrophys. **11**, 369 (2011).
[5] R. Stiskalek, J. Veitch, and C. Messenger, Mon. Not. R. Astron. Soc. **501**, 970 (2020).
[6] C. Caprini and D. G. Figueroa, Classical Quantum Gravity **35**, 163001 (2018).
[7] P. Auclair *et al.*, Living Rev. Relativity **26**, 5 (2023).
[8] N. Bartolo, D. Bertacca, R. Caldwell, C. R. Contaldi, G. Cusin, V. D. Luca, E. Dimastrogiovanni, M. Fasiello, D. G. Figueroa, G. Franciolini *et al.*, J. Cosmol. Astropart. Phys. 11 (2022) 009.
[9] A. C. Jenkins, M. Sakellariadou, T. Regimbau, and E. Slezak, Phys. Rev. D **98**, 063501 (2018).
[10] G. Cusin, C. Pitrou, and J.-P. Uzan, Phys. Rev. D **96**, 103019 (2017).
[11] G. Cusin, I. Dvorkin, C. Pitrou, and J.-P. Uzan, Phys. Rev. Lett. **120**, 231101 (2018).
[12] L. Valbusa Dall'Armi, A. Ricciardone, N. Bartolo, D. Bertacca, and S. Matarrese, Phys. Rev. D **103**, 023522 (2021).
[13] L. Amalberti, N. Bartolo, and A. Ricciardone, Phys. Rev. D **105**, 064033 (2022).
[14] L. Valbusa Dall'Armi, A. Ricciardone, and D. Bertacca, J. Cosmol. Astropart. Phys. 11 (2022) 040.
[15] A. Ricciardone, L. V. Dall'Armi, N. Bartolo, D. Bertacca, M. Liguori, and S. Matarrese, Phys. Rev. Lett. **127**, 271301 (2021).

[16] P. Adshead, N. Afshordi, E. Dimastrogiovanni, M. Fasiello, E. A. Lim, and G. Tasinato, Phys. Rev. D **103**, 023532 (2021).

[17] C. R. Contaldi, Phys. Lett. B **771**, 9 (2017).

[18] N. Bartolo, D. Bertacca, S. Matarrese, M. Peloso, A. Ricciardone, A. Riotto, and G. Tasinato, Phys. Rev. D **100**, 121501(R) (2019).

[19] B. P. Abbott (LIGO Scientific Collaboration and Virgo Collaboration), Phys. Rev. Lett. **120**, 091101 (2018).

[20] B. Allen and A. C. Ottewill, Phys. Rev. D **56**, 545 (1997).

[21] J. Aasi, B. P. Abbott, R. Abbott, T. Abbott, M. R. Abernathy, K. Ackley, C. Adams, T. Adams, P. Addesso *et al.* (The LIGO Scientific Collaboration), Classical Quantum Gravity **32**, 074001 (2015).

[22] F. Acernese, M. Agathos, K. Agatsuma, D. Aisa, N. Allemandou, A. Allocca, J. Amarni, P. Astone, G. Balestri, G. Ballardin *et al.*, Classical Quantum Gravity **32**, 024001 (2014).

[23] T. Akutsu, M. Ando, K. Arai, Y. Arai, S. Araki, A. Araya, N. Aritomi, H. Asada, Y. Aso, S. Bae *et al.*, Prog. Theor. Exp. Phys. **2021**, 05A102 (2021).

[24] M. Maggiore, C. Van Den Broeck, N. Bartolo, E. Belgacem, D. Bertacca, M. A. Bizouard, M. Branchesi, S. Clesse, S. Foffa, J. García-Bellido *et al.*, J. Cosmol. Astropart. Phys. 03 (2020) 50.

[25] M. Evans, R. X. Adhikari, C. Afle, S. W. Ballmer, S. Biscoveanu, S. Borhanian, D. A. Brown, Y. Chen, R. Eisenstein, A. Gruson *et al.*, arXiv:2109.09882.

[26] M. Maggiore, *Gravitational Waves. Vol. 1: Theory and Experiments* (Oxford University Press, New York, 2007), ISBN 978-0-19-171766-6, 978-0-19-852074-0.

[27] G. Mentasti and M. Peloso, J. Cosmol. Astropart. Phys. 03 (2021) 080.

[28] G. Mentasti, C. Contaldi, and M. Peloso, J. Cosmol. Astropart. Phys. 08 (2023) 053.

[29] A. A. Starobinskii, ZhETF Pisma Redaktsiiu **30**, 719 (1979), http://www.astrosurf.com/luxorion/Physique/starobinsky-inflation-jetp-1979.pdf.

[30] N. Bartolo, D. Bertacca, V. De Luca, G. Franciolini, S. Matarrese, M. Peloso, A. Ricciardone, A. Riotto, and G. Tasinato, J. Cosmol. Astropart. Phys. 02 (2020) 028.

[31] E. Dimastrogiovanni, M. Fasiello, A. Malhotra, P. D. Meerburg, and G. Orlando, J. Cosmol. Astropart. Phys. 02 (2022) 040.

[32] S. Kumar, R. Sundrum, and Y. Tsai, J. High Energy Phys. 11 (2021) 107.

[33] A. Malhotra, E. Dimastrogiovanni, G. Domènech, M. Fasiello, and G. Tasinato, Phys. Rev. D **107**, 103502 (2023).

[34] G. Cusin, I. Dvorkin, C. Pitrou, and J.-P. Uzan, Phys. Rev. D **100**, 063004 (2019).

[35] N. Bellomo, D. Bertacca, A. C. Jenkins, S. Matarrese, A. Raccanelli, T. Regimbau, A. Ricciardone, and M. Sakellariadou, J. Cosmol. Astropart. Phys. 06 (2022) 030.

[36] I. K. Wehus, U. Fuskeland, H. K. Eriksen, A. J. Banday, C. Dickinson, T. Ghosh, K. M. Górski, C. R. Lawrence, J. P. Leahy, D. Maino *et al.*, Astron. Astrophys. **597**, A131 (2017).

[37] P. D. Group, P. A. Zyla, R. M. Barnett, J. Beringer, O. Dahl, D. A. Dwyer, D. E. Groom, C. J. Lin, K. S. Lugovsky, E. Pianori *et al.*, Prog. Theor. Exp. Phys. **2020**, 083C01 (2020).